

# Sensorless Reduction of Cane Oscillations Aimed at Improving Robotic Grapevine Winter Pruning

Andrea Fimiani<sup>1</sup><sup>a</sup>, Pierluigi Arpentì<sup>1</sup><sup>b</sup>, Matteo Gatti<sup>2</sup><sup>c</sup> and Fabio Ruggiero<sup>1</sup><sup>d</sup>

<sup>1</sup>*Dip. di Ingeg. Elet. e Tecn. dell'Inform., Università degli Studi di Napoli Federico II, Via Claudio 21, Napoli, Italy*

<sup>2</sup>*Dipartimento di Scienze delle Produzioni Vegetali Sostenibili, Università Cattolica del Sacro Cuore, Piacenza, Italy*  
fi

**Keywords:** Agricultural Automation, Robotic Pruning, Momentum-Based Observer.


**Abstract:** Agricultural sector faces challenges like high labour costs and a shortage of qualified workers for repetitive tasks, leading to increased interest in agricultural robotics. Pruning is a focus for automation efforts worldwide. However, pruning robots struggle with slow and inaccurate vision systems, resulting in slow, costly, and potentially harmful operations for plants. This study aims to provide a reproducible and reliable method for detecting contact with grapevines during pruning, minimising potential damage, and improving vision system speed by reducing cane oscillations. The proposed approach uses a momentum-based observer, eliminating the need for force sensors. Experiments on *Vitis vinifera* cv. Pinot Noir canes validated this methodology.


## 1 INTRODUCTION


Grapevine winter pruning is an essential practice that must be performed annually over dormancy. From a viticulture perspective, it holds great significance as it profoundly impacts various aspects of vine growth, yield, and fruit quality (Poni et al., 2018). Pruning grapevines differs from pruning other fruit trees for several reasons encompassing distinctive plant morphology, bud fruitfulness, and training systems. Indeed, it involves making specific cuts on dormant grapevines aimed at removing part of the previous season's growth as well as retaining selected dormant shoots, namely, canes and spurs (Poni et al., 2016). Pruning requires the pruner's ability to quickly recognise and locate cutting points in narrow spaces despite cane density and other trellis accessories that may obstruct vision (Guadagna et al., 2023). Due to the intrinsic complexity of the task, robotising grapevine winter pruning requires a multidisciplinary approach to address challenges ranging from cutting point identification to path planning in a cluttered environment and cane collision detection (Epee et al., 2022). Cameras often have lengthy processing times and may provide inaccurate position estimates, causing ineffi-


ciencies in pruning tasks and the risk of plant damage. This limitation remains a significant hurdle in robotics, especially for pruning (Zahid et al., 2021). While improving position estimation algorithms can enhance accuracy, it is not always feasible due to atmospheric conditions and obstructed camera views. Another challenge arises from pruning-induced oscillations caused by manipulator-cane collisions and cutting. These oscillations worsen when the manipulator applies unnecessary force to the cane, resulting from inaccurate node position estimation. This excess force can bend the vine due to its rigid support and elastic cane material. After trimming, the plant starts oscillating, potentially damaging it and slowing down the vision system, impacting productivity. The oscillation issue is addressed by rapidly detecting collisions between the shear centre and the trim point, preventing the robot from unnecessary vine pushing. Collision detection strategies can adapt to context and application, but traditional methods involve expensive force sensors and robot's end-effector modifications. Building upon these developments, this paper aims to reduce cane oscillations induced by the collisions occurring during pruning, relying on measures retrieved from proprioceptive sensors only.

This paper introduces a novel approach, leveraging a momentum-based observer (De Luca et al., 2006) for collision detection in precision viticulture, specifically in grapevine winter pruning. To the best of our knowledge, this is the first application of the

<sup>a</sup> <https://orcid.org/0009-0006-4452-0106>

<sup>b</sup> <https://orcid.org/0000-0002-0327-3069>

<sup>c</sup> <https://orcid.org/0000-0003-4195-7709>

<sup>d</sup> <https://orcid.org/0000-0001-7539-9157>

momentum-based observer in this context, addressing collisions occurring before and after the expected cutting point. This work focuses on the former to minimize cane pushing and oscillations. The latter is crucial to avoid false cuts that could slow down the pruning process, and it is not deepened in this work.

Additionally, the paper enhances system reproducibility and reliability by proposing an affordable, customised electromechanical setup compatible with off-the-shelf commercial shears, eliminating the need for specialised equipment.

The paper's outline is: Section 2 revises the available solutions for robot pruning; Section 3 presents the collision management framework; an extensive experimental campaign is proposed in Section 4, showing that the momentum-based observer prevents the manipulator from damaging the vine and inducing low amplitude oscillations; conclusions are supported by the statistical analysis presented in Section 4.4, based on the metrics described in Section 4.3; Section 5 concludes the paper.

## 2 LITERATURE REVIEW

A comprehensive perception system is often required to understand the plant's structure and make informed-cutting decisions. A vision system that reconstructs the tree canopy in 3D, identifies retained canes and pruning decisions, calculates pruning point coordinates, and plans collision-free paths, has been proposed for cane pruning (Botterill et al., 2017). On the other hand, some robotic systems incorporate vision sensors mounted on the manipulator's arm. For instance, an approach that utilises an RGB-D camera and custom pneumatic shears as the cutting tool has been developed (You et al., 2020). Recently, a deep learning-based methodology for pruning region detection and canopy segmentation of mature spur-pruned grapevines has been proposed (Guadagna et al., 2023). A multi-modular framework that combines deep learning, computer vision, and robot control for dynamic and reproducible pruning skills has been proposed (Katyara et al., 2020). A notable example of a robot involved in grapevine pruning is the *Rolling Panda* (Teng et al., 2021). It is a wheeled mobile manipulator system consisting of a non-holonomic wheeled mobile platform and a seven degrees-of-freedom (DoF) robotic arm, incorporating a hierarchical control strategy that prioritises the desired path while considering other constraints using the *stack-of-tasks* framework. While initially designed to enhance safety in human-robot interaction scenarios, the momentum-based observer employed

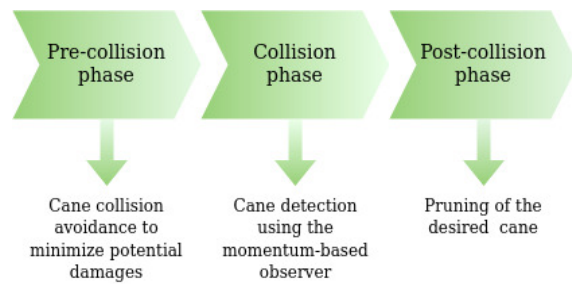


Figure 1: Collision management diagram.

in this paper has been successfully adapted to diverse robotic systems and situations. For instance, in the field of legged robots, it has been used to estimate external disturbances acting on the legs of a quadrupedal robot (Morlando et al., 2021) or to accurately localise external contacts on an Atlas robot using a contact particle filter (Manuelli and Tedrake, 2016). In aerial robotics, the momentum-based observer has been employed on fully actuated aerial robots to estimate external contact forces during physically interactive aerial tasks (Ryll et al., 2017). Notably, it has been further enhanced by using a higher-order estimator for estimating external wrenches in the decentralised control of aerial robotic manipulators (Ruggero et al., 2015).

## 3 COLLISIONS MANAGEMENT

Collision management techniques developed for robot-human collisions can also be applied to manage robot-cane collisions. Collision events can be divided into three main phases, namely *pre-collision phase*, *collision phase*, and *post-collision phase*, as synthetically depicted in Fig. 1. The pre-collision phase regards the design of an appropriate path planning algorithm to quickly generate the trajectory as the environment changes with each cut, based on the extensive use of exteroceptive sensors, such as cameras or range sensors. These arguments, briefly revised in Section 2, are out of the scope of the presented work and, thus, will not be further deepened.

The collision phase is the second phase of the collision handling process, and its primary goal is to rapidly detect the occurrence of the collision between the shears mounted on the manipulator's end-effector and the cane while gathering as much information as possible from the impact forces. It is important to note that the collision phase can be complex and requires careful design and implementation. Particular attention should be given to the accuracy and timeliness of collision detection, as well as the robustness of the system in avoiding false pos-

itives. This paper proposes to manage the collision between the shear and the vine using an  $n^{\text{th}}$ -order momentum-based observer. The momentum-based observer (De Luca et al., 2006) is a reliable collision detection method to enhance safety in human-robot interaction scenarios. The approach based on the generalised momentum is widely used since it avoids the calculation of acceleration that introduces noise and delay. Indeed, this method relies on the available model knowledge, the last commanded torques, and the signals retrieved from proprioceptive position sensors to estimate the lumped effect of all unmodelled terms (interaction with the environment, disturbances, effects from model uncertainties, etc.) as joint torque  $\tau_e$ . Considering a rigid-link manipulator with  $n > 0$  joints, the dynamic model of n-DoF robot manipulators is presented as follows

$$M(q)\ddot{q} + C(q, \dot{q})\dot{q} + g(q) = \tau_{tot}, \quad (1)$$

where the matrices  $M(q) \succ 0 \in \mathbb{R}^{n \times n}$ ,  $C(q, \dot{q}) \in \mathbb{R}^{n \times n}$ , and  $g(q) \in \mathbb{R}^n$  represent the inertia matrix, Coriolis and centrifugal terms matrix, and gravity vector, respectively. The symbol  $\succ 0$  indicates that the related matrix is positive-definite. Vectors  $q, \dot{q}, \ddot{q} \in \mathbb{R}^n$  represent the joint angular position, velocity, and acceleration, respectively, while  $\tau_{tot} \in \mathbb{R}^n$  represents the total torque acting on each joint actuator. This total torque can be divided into two components, namely  $\tau \in \mathbb{R}^n$ , which represents the input torques commanded to the joint actuators and  $\tau_e \in \mathbb{R}^n$ , which represents the external joint torque acting on them. Define the generalised momentum of the system as  $p = M(q)\dot{q} \in \mathbb{R}^n$ . Because of the skew-symmetry property of the inertia matrix, namely  $\dot{M}(q) = C(q, \dot{q}) + C^T(q, \dot{q})$ , the following

$$\dot{p} = \tau_{tot} + C^T(q, \dot{q})\dot{q} - g(q) \quad (2)$$

holds. The derivation of the classic first-order momentum observer is based on the following definition of the collision detection signal  $r(t) = K_I \left[ p(t) - \int_0^t (\tau + C^T(q, \dot{q})\dot{q} - g(q) + r) ds - p(0) \right]$ , where  $p(0)$  is the value of the momentum at time  $t = 0$  s, and  $K_I \succ 0 \in \mathbb{R}^{n \times n}$  is a diagonal gain matrix. Using (2) and the dynamic model in (1), the following expression is derived

$$\dot{r} = -K_I r + K_I \tau_e. \quad (3)$$

When a collision occurs, the signal  $r$  exhibits exponential growth and collision detection can be achieved by comparing it to a threshold value  $r_{low}$  determined based on the system's noise characteristics. In ideal conditions, as the gain  $K_I$  tends to infinity, the signal  $r$  closely approximates the external torques acting on the manipulator  $\tau_e$ . Therefore, higher gains are preferable to enhance the sensitivity of collision detection.

Due to its properties, the signal  $r$  can infer the external forces  $f_{ext}$  exerted on the end effector of the manipulator. Indicating with  $\dagger$  the left pseudo-inverse of a given matrix, it is possible to write  $r \approx \tau_e = J^T F_{ext} \Rightarrow f_{ext} = (J^T)^\dagger r$ . The dynamics of the collision identification signal in (3) can be studied component-wise in the Laplace domain as  $\frac{r_j(s)}{\tau_{e,j}(s)} = \frac{K_{I,j}}{s + K_{I,j}}$  with  $j = 1, \dots, n$ . These transfer functions represent first-order systems with a negative real-part pole at  $-K_{I,j}$ . The negative pole ensures the collision identification signal  $r_j$  convergence towards  $\tau_{e,j}$  at steady-state. To achieve a more accurate and precise collision detection response and to mitigate the impact of high-frequency noise, a second-order observer can be designed by assuming a linear relationship between external forces and their estimation in the Laplace domain. This can be achieved by employing a second-

order transfer function as  $T_i(s) = \frac{\omega_{n,i}^2}{s^2 + 2\zeta_i \omega_{n,i} s + \omega_{n,i}^2}$

with  $i = 1, \dots, n$ , where  $\omega_{n,i}$  and  $\zeta_i$  are the desired natural frequency and damping of the designed estimator, respectively. To achieve the desired transfer function, the collision identification signal can be expressed in the time domain as  $r(t) = K_1 \int_0^t -r(s) + K_2 \left[ q(s) - \int_0^t (\tau + C^T(q, \dot{q})\dot{q} - g(q) + r) ds - p(0) \right] ds$ , where it is assumed that  $q(0) = r(0) = \dot{r}(0) = 0$ , while  $K_1 \succ 0 \in \mathbb{R}^{n \times n}$  and  $K_2 \succ 0 \in \mathbb{R}^{n \times n}$  are diagonal matrices. Generalising the above reasoning, it is possible to extend the discussion to an  $n^{\text{th}}$ -order estimator, which is described by the following detection signal (Morlando et al., 2021)  $\gamma_i(t) = K_i \int_0^t -r + \gamma_{i-1} ds$ , with  $i = 2, \dots, n$ , and where  $\prod_{i=j+1}^n K_i = c_j$  with  $j = 0, \dots, n-1$  and  $c_j$  represents the coefficients in the denominator of the desired transfer function.

For the specific task of this paper, the detection of a collision serves as a triggering signal to start pruning. The cutting process has to fulfil specific pre-determined requirements.

- **Reduction of Cane Deflection.** During pruning, it is crucial not to compromise the integrity of the vine cane.
- **Fast Trim Point Recognition.** Cutting each trim point has to be performed in such a way as to speed up the overall pruning process.
- **Cost-Effective Solution.** The robotic system must be easily adaptable to any pruning requirement and must increase production.

To meet the above functional requirements, it is necessary to establish appropriate metrics that capture the cutting process's effects on vine dynamics.

## 4 EXPERIMENTAL VALIDATION

An experimental campaign was carried out, involving cuts made both with and without the momentum-based observer, aimed at demonstrating the effectiveness of the presented method. Furthermore, since plant health is another aspect of considerable importance in commercial vineyards, the cutting angle adopted is critical. For this reason, a greater cut inclination angle is more effective in reducing the accumulation of humidity on the pruning cuts. For this reason, the effectiveness of the methodologies is evaluated by considering two scenarios: cutting parallel to the ground and cutting at an angle of 45 degrees with respect to the ground. The performed experiments can be divided into four classes.

- **Off–0.** Cuts are made without using the momentum-based observer, with a cutting plane parallel to the ground.
- **Off–45.** Cuts are made without using the momentum-based observer, with a cutting plane inclined by 45 degrees with respect to the ground.
- **On–0.** Cuts are made using the momentum-based observer, with a cutting plane parallel to the ground.
- **On–45.** Cuts are made using the momentum-based observer, with a cutting plane inclined by 45 degrees with respect to the ground.

A video summarising the carried out experiments can be found at <https://youtu.be/nFbt2YoQUqc>.

### 4.1 Experimental Setup

During the experimental campaign, the KUKA LBR iiwa7 R800 robot arm was used. Professional electronic shears (textitVinion 250) were used for pruning. To attach these shears to the robot's flange, a support was designed and printed using CAD modeling (Fig. 2). This support includes an Arduino Nano connected to a stepper motor, positioned to control the shear trigger's opening and closing.

To accurately measure oscillations at high frequencies and millimeter-level amplitudes, a reliable ground truth system was needed. The AprilTag2 system (Wang and Olson, 2016), specifically tags from the tag36h11 family, was used. To minimise the oscillation of the canes and allow an improvement in the identification times of the upstream visual system, the tags were fixed on the canes different from the one in contact with the shears, that is, the one to which the trim point belongs, to measure how the cutting process influences the movement of the vine. Two square tags measuring 0.08 m for each side were used

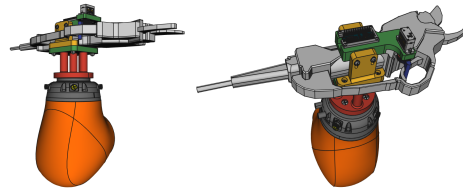


Figure 2: 3D CAD model of the tool mounted on the end-effector of the KUKA LBR iiwa7 R800 manipulator.

on the canes, and one square tag measuring 0.1 m for each side was fixed on the cord. All the case studies were carried out using two vines of *Vitis vinifera* L. cv. Pinot Noir collected right after pruning operations and stored at 10 °C. The samples were bound to a steel-made structure which made it possible to replicate the same orientation assumed by vines in actual vineyards, guaranteeing robustness for the pruning process and preventing the structure from sliding during the manipulator-cane contact. To achieve a good compromise between detection accuracy and responsiveness, a fourth-order momentum-based observer has been utilised with gains  $K_1 = 10I_7$ ,  $K_2 = 20I_7$ ,  $K_3 = 30I_7$ ,  $K_4 = 40I_7$  where  $I_7$  is the identity matrix of proper dimensions. Since the collision signal relies entirely on model knowledge, issues arise from model uncertainty, yielding the momentum-based observer to supply non-zero collision signals even in the absence of a collision (i.e., false positives). A false positive represents uncertainty about the effective presence of the vine cane in the cutting area of the shear. A given threshold for collision signals has been thus defined. The threshold was chosen empirically by comparing forces detected due to movements without collisions (free motion) and those detected during the collision with a vine cane. During the analysis, the estimated forces along the axis approaching the vineyard, i.e., the  $x$ -axis, were more indicative of the possible presence of a collision. Observing increased forces along the  $x$ -axis direction during collision prompted a specific focus on these forces. Several tests found that the estimated external force at the tip before initiating movement oscillated within the range of [0.5, 1.5] N. Conversely, the minimum values consistently remained within  $[-1.10, -1.23]$  N during free motion. Therefore, a force threshold of  $-1.3$  N was selected as it was never exceeded during non-colliding movements. Besides, implementing the momentum observer on the robot introduces higher noise levels. The use of position encoders to recover speed information introduces noise. Therefore, a third-order Butterworth filter was employed to generate filtered collision detection signals, further reducing false positives.

## 4.2 The Pruning Experiment

The sequence of events characterising the experimental validation begins with the manipulator receiving the estimated position for the trim point, to be reached at time  $t_{ip}$ . The trajectory planner provides the desired position based on the data gathered by the external camera system. The camera system exploited in the literature to detect the buds on the canes is generally distinct from the system employed here as ground truth to track tags' motion. Due to an incorrect estimation of the cane position retrieved by vision, the shears collide with the vine earlier or later than expected, pushing the cane away from its initial rest position, denoted as  $x_0$ , at  $t = 0$ . Through a 4-th order momentum-based observer, the proposed framework detects the collision signal due to contact with the cane at time  $t_{cs}$  and stops the manipulator. Notice that  $t_{cs}$  is not the actual time at which the shear collides with the cane but the time at which the observer detects the collision. Therefore if  $t_{co}$  is the actual contact time, it will always be  $t_{cs} \geq t_{co}$  where the time lag  $t_{lag} = t_{cs} - t_{co} \geq 0$  depends upon the order of the momentum-observer, the order of the Butterworth filter, and the elastic properties of the cane. If  $t_{cs} \leq t_{ip}$ , the framework stops the manipulator before reaching the planned position at  $t_{ip}$ , preventing potential damages to the vine. If  $t_{cs} \geq t_{ip}$ , the framework keeps moving along the same approach direction until a collision signal is detected. It has been supposed that the estimated positions of the trim points, which are retrieved by the vision system, are always further compared to the actual positions of the nodes and that they are aligned along the approach direction of the end-effector, that is  $t_{cs} \leq t_{ip}$  always. Then, the shears initiate the cutting command, which takes  $\approx 2.1$  s to cut the vine cane. The whole experimental setup, as well as, two distinct moments of the experiment described until this point have been captured and shown in Fig. 3, namely, the manipulator approaching the vine and the shears preparing to cut the cane. At the instant  $t_{cut}$ , the cane is free to move and begins to perform a damped oscillatory motion around its final rest position  $x_f$ , which is reached at the instant  $t_f$ .

## 4.3 Pruning Metrics

Several metrics are considered and introduced to validate the effectiveness of the proposed methodologies.

The first metric identified is the displacement from the initial position, denoted as  $\Delta$ . It measures the difference between the cane position at the instant preceding the cutting procedure start,  $t_{cs}$ , and its initial position at time  $t = 0$ , denoted as  $x_0$ , that is

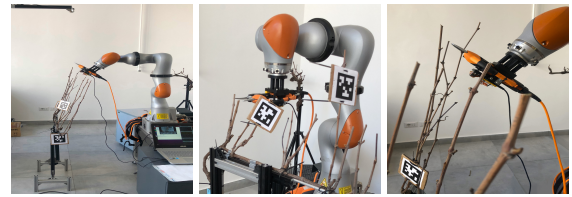


Figure 3: Cutting of grapevine canes via Pellenc Vinion 250 shears mounted on the KUKA LBR iiwa7 R800 robot. Left: the experimental setup is presented. Centre: the manipulator is approaching the cane. Right: a cut with an approach angle of 45 degrees.

$$\Delta = x(t_{cs}) - x_0.$$

The second metric describes the amplitude of the oscillations,  $A$ . This is the magnitude of the first oscillation exhibited by the plant immediately after the cut, computed as the difference between the maximum and minimum measured positions of the cane between the cutting time  $t_{cut}$  and the final rest position  $x_f$  at time  $t_f$ , that is  $A = \max\{x(t)\} - \min\{x(t)\}$ , with  $t \in [t_{cut}, t_f]$ , where  $\max\{x(t)\}$  and  $\min\{x(t)\}$  are considered with respect to the cane's rest position, treated as zero reference position.

The third metric is the settling time,  $T_a$ , representing the time required for the cane position to stabilise at its final position  $x_f$ . The final position is reached in the instant  $t_\epsilon$ , beyond which the difference between the actual and final positions is below  $\epsilon = 1\%$  of its final position. Notice that the position signal was first filtered to prevent noise from affecting the measurement, that is

$$T_a = t_\epsilon - t_{cut}, \text{ where } t_\epsilon = \sup\{t \in \mathbb{R}^n \mid \|x(t) - x_f\| \geq 0.01\epsilon x_f\}.$$

Finally, the normalised signal energy  $E = \frac{1}{T_a} \int_{t_{cut}}^{t_\epsilon} |x(t)|^2 dt$  is proposed as the fourth metric. Due to the relationship between the notion of energy of a signal in signal processing and the notion of energy in physics (Kaiser, 1990), signal energy has been chosen as a qualitative indicator of the energy exchanged between the manipulator with the electronic shears and the vine during pruning. Since the two proposed cutting schemes,  $On - 0$  and  $On - 45$ , require different time intervals to perform each cut, the time interval of the cut has normalised the energy signal.

All the above metrics are synthetically listed in Table 1 and provide a comprehensive framework for assessing the fulfilment of the established requirements and objectives. Without information regarding the canes' dynamic behaviour, it was impossible to establish specific target values for the presented metrics. Nevertheless, it is desirable to obtain a reduction of the displacement from the rest position to ensure less stress on the grapevine canes. This reduction is expected to significantly impact the oscillation am-

Table 1: Metrics characterising pruning.

Metrics	Description	Units
$\Delta$	displacement from rest position	[m]
$A$	oscillations amplitude	[m]
$T_a$	settling time	[s]
$E$	normalised signal energy	[m <sup>2</sup> ]

plitude, which needs to be minimised to expedite the identification of subsequent trim points by any external vision-based system. To evaluate and compare the methodologies, the temporal trends of several canes' positions were measured using tags, as seen in Section 4.1. As a preliminary assessment of the proposed methodology, the cases  $Off - 0$  and  $On - 0$  are depicted in Fig.4. Both case studies were performed by cutting the cane on which the tag was affixed (the trim point is located at the 10-th node while the tag is mounted at the 3-rd one), and for this reason, they can clearly show a significant improvement in the approach to the single cane. It can be immediately stated that, when the momentum-based observer is not deployed, the maximum displacement of the tag from the rest position is  $\Delta \approx 0.008$  m and the amplitude oscillations are  $A \approx 0.04$  m. When the observer is deployed, the maximum displacement of the tag is  $\Delta \approx 0.004$  m, and the amplitude oscillation is  $A \approx 0.005$  m. Therefore, these preliminary results show a decrement of the amplitude of the oscillations of one order of magnitude in the case  $On - 0$  compared to the  $Off - 0$ , resulting in an overall reduction of the vine's mechanical stress. The settling time is strongly linked to the structural and material characteristics of the system and is inversely proportional to the system damping coefficient. A shorter settling time implies a shorter oscillation duration, leading to faster processing times. However, the damping coefficient exhibits a nonlinear behaviour and increases with the applied excitation forces (Amabili, 2018). Given the primary objective of reducing excitation forces, the settling time is expected to increase, but preferably only to a small extent. Finally, the normalised signal energy provides information about the energy involved in the cutting process; therefore, it is expected to be smaller with the momentum-based observer. All the developed methodologies were tested through a measurement campaign and subsequent statistical analysis to assess their advantages.

#### 4.4 Statistical Analysis and Discussion

Cane properties vary due to environmental factors, leading to differences in size, shape, internode length, and other characteristics, even within the same vine.

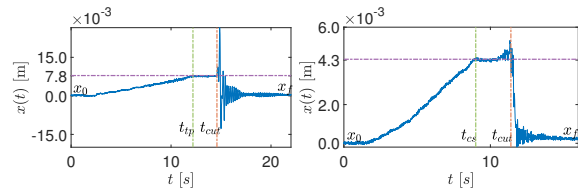


Figure 4: Time evolution of the tag positions. Left: the observer is not deployed ( $Off - 0$ ); the end-effector reaches the planned point at  $t_{tp} \approx 12.5$  s; the cane is trimmed after 2.1 s. Right: the observer is exploited ( $On - 0$ ); the collision signal is detected at  $t_{cs} \approx 9$  s. Oscillations on the left have larger values for  $\Delta$  and  $A$  compared to the right image.

Thus, comparing pruning methods requires conducting enough cutting operations to showcase the benefits of one technique over another. For the following analysis, 200 cuts were performed on two Pinot Noir grapevines, from the 13-th node down to the 2-nd. The sequence of cutting approaches has been randomly generated among the four proposed scenarios, namely,  $Off - 0$ ,  $Off - 45$ ,  $On - 0$ , and  $On - 45$ . The worst-case scenario was assumed, where the vision algorithm had a cut position error of 0.04 m. As a result, the manipulator received a position command that anticipated a forward movement of 0.2 m, while the actual position of the cane was 0.16 m away. The positioning trend of the tags was extracted from the 200 videos using a Python-based ROS launch file and subsequently analysed using the Matlab platform.

A complete statistical analysis has been carried out to validate the methodology proposed. The defined metrics allow the definition of a sampling distribution closely related to the probability distribution of the sample and to the descriptive model of the population. In particular, indicating the sample size with  $N$ , each metric is described through the sample arithmetic mean  $\mu = \frac{1}{N} \sum_{j=1}^N x_j$  and the standard error  $\sigma_x = \frac{\sigma}{\sqrt{N}}$  of the mean (standard error), where  $x_j$  is the  $j$ -th sample with  $j = 1, \dots, N$ , and  $\sigma = \sqrt{\sigma^2}$  is the standard deviation with variance  $\sigma^2 = \frac{1}{N-1} \sum_{j=1}^N |x_j - \mu|^2$ .

Some tests were conducted to explore reducing cutting forces by adjusting cutting speed. A servo motor, controlled by an Arduino Nano, managed the shears' closure. Two cases were examined to minimize cutting-induced oscillations. First, a rapid and decisive cut was executed by commanding the servo motor to fully close the trigger in a single motion, taking 1.5 s. The second case involved a slower trigger motion, where the servo motor was gradually commanded to different positions, taking 2.1 s. The manipulator was fixed, with the plane of the shear blades parallel to the floor, and all cuts were made between the fourth and fifth nodes. Ten oscillations resulting from the two cutting methods were measured, and a

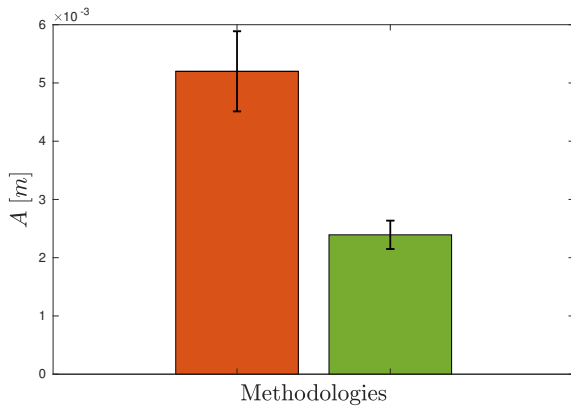


Figure 5: Mean and standard error of the cutting-induced oscillations amplitude  $A$  on the Pinot Noir: sharp cut (red) and controlled cut (green).

statistical analysis was performed. The mean and the standard error of the measured oscillations amplitude  $A$ , represented in Fig. 5, demonstrate a significant difference in the two cutting typologies. Considering the project's objective of minimising oscillations to reduce the processing time of vision algorithms, the trade-off between reducing oscillations solely caused by cutting force and the additional 0.6 s in cutting time was deemed highly beneficial. Consequently, the cuts for the four methodologies were performed using the second method, assuming similar results for the cuts made at 45 degrees, with slightly higher averages due to the bigger cutting surface.

Regarding the displacement from the rest position, in Fig. 6 (top left), it is possible to appreciate the effectiveness of the proposed methods. The  $On-0$  case has an average displacement of 0.2 mm, with an effective displacement reduction of 87.2% compared to the  $Off-0$  case. Similarly, the case  $On-45$  has an 81.9% reduction compared to the case  $Off-0$ . Note that both average values are affected by a very low standard error and that the  $On-45$  case also performs 70.4% better than the  $Off-0$  case. Table 2 (top left) synthesises the above results.

The vine oscillation is influenced by forces due to the contact between the shears and the cane and forces resulting from cutting. While these factors contribute to the overall oscillation, the displacement of the vine cane plays a crucial role in determining the amplitude of the oscillation. Figure 6 (top right) shows that the oscillations in the  $On-0$  and  $On-45$  cases achieve a reduction of 69.1% and 51.6% respectively, compared to the  $Off-0$  and  $Off-45$  cases. As reported in Table 2 (top right), the average oscillation is reduced to  $\approx 0.002$  m and 0.003 m in the  $On-0$  and  $On-45$  cases, respectively, with very low standard error. These results demonstrate the effectiveness of

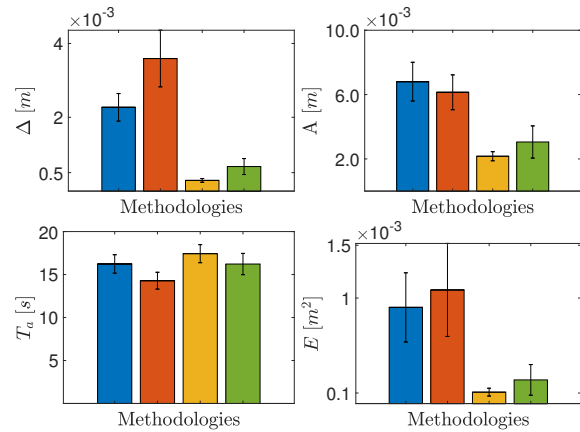


Figure 6: Mean and standard error: displacement from the rest position (top left), oscillation amplitude (top right), settling time (bottom left), normalised signal energy (bottom right). Blue:  $Off-0$  case, red:  $Off-45$  case, yellow:  $On-0$  case, green:  $On-45$  case.

Table 2: Mean and standard error: displacement from the rest position (top left), oscillation amplitude (top right), settling time (bottom left), normalised signal energy (bottom right).

Case Study	$\Delta$		$A$	
	$\mu$ [m]	$\sigma_x$ [m]	$\mu$ [m]	$\sigma_x$ [m]
$Off-0$	$2.2 \times 10^{-3}$	$3.7 \times 10^{-4}$	$6.8 \times 10^{-3}$	$1.2 \times 10^{-4}$
$Off-45$	$3.6 \times 10^{-3}$	$7.5 \times 10^{-4}$	$6.2 \times 10^{-3}$	$1.0 \times 10^{-4}$
$On-0$	$2.8 \times 10^{-4}$	$0.5 \times 10^{-4}$	$2.1 \times 10^{-3}$	$2.8 \times 10^{-4}$
$On-45$	$6.5 \times 10^{-4}$	$2.1 \times 10^{-4}$	$3.0 \times 10^{-3}$	$9.8 \times 10^{-4}$

Case Study	$T_a$		$E$	
	$\mu$ [m]	$\sigma_x$ [m]	$\mu$ [m]	$\sigma_x$ [m]
$Off-0$	16.23	1.07	$0.9 \times 10^{-3}$	$0.3 \times 10^{-3}$
$Off-45$	14.24	0.96	$1.0 \times 10^{-3}$	$0.4 \times 10^{-3}$
$On-0$	17.43	1.05	$0.1 \times 10^{-3}$	$0.3 \times 10^{-4}$
$On-45$	16.50	1.23	$0.2 \times 10^{-3}$	$0.1 \times 10^{-3}$

the proposed methods in reducing the amplitude of the oscillations in both cases.

Figure 6 (bottom left) and Table 2 (bottom left) show the average settling times between 14 and 17 s. This variability is likely due to the heterogeneity of the vine's mechanical properties. The average of the cases  $On-0$  and  $On-45$  is slightly higher than the tests carried out without the observer. However, given the high standard error of the data, an almost equal settling time for all methodologies can be assumed.

Figure 6 (bottom right) shows that the proposed methodologies significantly reduce the normalised signal energy. Table 2 (bottom right) states that the cases  $On-0$  and  $On-45$  exhibit a reduction in  $E$  by 88.8% and 80%, respectively. This reduction may indicate that, during cutting, a lower amount of energy is involved, which potentially means less alteration of the system's initial state.

## 5 CONCLUSION

This paper introduced a force-sensor-free methodology to reduce grapevine cane oscillations during robotic winter pruning. It relied on the momentum-based observer algorithm and used proprioceptive sensors for external force feedback. Experimental testing, with 200 randomised cuts on Pinot Noir grapevines using a KUKA LBR iiwa7 manipulator with a commercial shear system, demonstrated a reduction in oscillation amplitudes, confirming the method's effectiveness. The goal is to create a cost-effective and easily reproducible robotic system to speed up winter pruning. In future, potential areas of improvement include controlling shear blade forces during cuts and integrating algorithms for optimising robot-plant interactions to improve vine cane pruning.

## ACKNOWLEDGEMENTS

The research leading to these results has been supported by both the PRINBOT project (in the frame of the PRIN 2017 research program, grant number 20172HHNK5 002) and the COWBOT project (in the frame of the PRIN 2020 research program, grant number 2020NH7EAZ.002). The authors are solely responsible for its content.

## REFERENCES

- Amabili, M. (2018). Nonlinear damping in large-amplitude vibrations: modelling and experiments. *Nonlinear Dynamics*, 93(1):5–18.
- Botterill, T., Paulin, S., Green, R., Williams, S., Lin, J., Saxton, V., Mills, S., Chen, X., and Corbett-Davies, S. (2017). A robot system for pruning grape vines. *Journal of Field Robotics*, 34(6):1100–1122.
- De Luca, A., Albu-Schaffer, A., Haddadin, S., and Hirzinger, G. (2006). Collision detection and safe reaction with the dlr-iii lightweight manipulator arm. In *2006 IEEE/RSJ International Conference on Intelligent Robots and Systems*, pages 1623–1630.
- Epee, P., Schelezki, O., Parker, A., Trought, M., Werner, A., Hofmann, R., Almond, P., and Fourie, J. (2022). Characterising retained dormant shoot attributes to support automated cane pruning on vitis vinifera l. cv. sauvignon blanc. *Australian Journal of Grape and Wine Research*, 28(3):508–520.
- Guadagna, P., Fernandes, M., Chen, F., Santamaria, A., Teng, T., Frioni, T., Caldwell, D. G., Poni, S., Semini, C., and Gatti, M. (2023). Using deep learning for pruning region detection and plant organ segmentation in dormant spur-pruned grapevines. *Precision Agriculture*.
- Kaiser, J. (1990). On a simple algorithm to calculate the 'energy' of a signal. In *International Conference on Acoustics, Speech, and Signal Processing*, pages 381–384 vol.1.
- Katyara, S., Ficuciello, F., Caldwell, D. G., Chen, F., and Siciliano, B. (2020). Reproducible pruning system on dynamic natural plants for field agricultural robots.
- Manuelli, L. and Tedrake, R. (2016). Localizing external contact using proprioceptive sensors: The contact particle filter. In *2016 IEEE/RSJ International Conference on Intelligent Robots and Systems (IROS)*, pages 5062–5069.
- Morlando, V., Teimoorzadeh, A., and Ruggiero, F. (2021). Whole-body control with disturbance rejection through a momentum-based observer for quadruped robots. *Mechanism and Machine Theory*, 164:104412.
- Poni, S., Gatti, M., Palliotti, A., Dai, Z., Duchêne, E., Truong, T.-T., Ferrara, G., Matarrese, A. M. S., Gallotta, A., Bellincontro, A., Mencarelli, F., and Tombesi, S. (2018). Grapevine quality: A multiple choice issue. *Scientia Horticulturae*, 234:445–462.
- Poni, S., Tombesi, S., Palliotti, A., Ughini, V., and Gatti, M. (2016). Mechanical winter pruning of grapevine: Physiological bases and applications. *Scientia Horticulturae*, 204:88–98.
- Ruggiero, F., Cacace, J., Sadeghian, H., and Lippiello, V. (2015). Passivity-based control of vtol uavs with a momentum-based estimator of external wrench and unmodeled dynamics. 72:139–151.
- Ryll, M., Muscio, G., Pierri, F., Cataldi, E., Antonelli, G., Caccavale, F., and Franchi, A. (2017). 6d physical interaction with a fully actuated aerial robot. In *2017 IEEE International Conference on Robotics and Automation (ICRA)*, pages 5190–5195.
- Teng, T., Fernandes, M., Gatti, M., Poni, S., Semini, C., Caldwell, D., and Chen, F. (2021). Whole-body control on non-holonomic mobile manipulation for grapevine winter pruning automation.
- Wang, J. and Olson, E. (2016). Apriltag 2: Efficient and robust fiducial detection. In *2016 IEEE/RSJ International Conference on Intelligent Robots and Systems (IROS)*, pages 4193–4198.
- You, A., Sukkar, F., Fitch, R., Karkee, M., and Davidson, J. R. (2020). An efficient planning and control framework for pruning fruit trees. In *2020 IEEE International Conference on Robotics and Automation (ICRA)*, pages 3930–3936.
- Zahid, A., Mahmud, M. S., He, L., Heinemann, P., Choi, D., and Schupp, J. (2021). Technological advancements towards developing a robotic pruner for apple trees: A review. *Computers and Electronics in Agriculture*, 189:106383.